Thesis for Master Degree

Variation of the Tropical Cyclone Season in the Western North Pacific

Advisor : Prof. Hyeong-Seog Kim

February 2017

Department of Convergence Study on the Ocean Science and Technology

School of Ocean Science and Technology
Korea Maritime and Ocean University

Donghee Kim

본 논문을 김동희의 이학석사 학위논문으로 인준함.

위원장 이 호 진 (인)

위 원 김 형 석 (인)

위 원 박 두 선 (인)

2016년 11월 24일

한국해양대학교 해양과학기술전문대학원

Contents

List of Tables

List of Figures

북서태평양 열대저기압 활동기간의 변화에 대한 연구

김 동 희

해양과학기술융합학과

한국해양대학교 해양과학기술전문대학원

요 약

북서태평양에서 열대저기압 활동기간은 이전 겨울철의 상대적인 해수면온도 분포와 관련이 있다. 열대저기압 활동기간의 길이는 그 시작일에 크게 의존하며 시작일은 이전 겨울철 인도양과 동태평양의 해수면온도에 의해 조절된다. 겨울과 이른 봄에 인도양과 동태평양의 해수면온도가 상대적으로 높으면 태풍발생지역인 북서태평양 부근에 고기압 아노말리가 강화되어 열대저기압의 발달을 억제하고 결과적으로 열대저기압 활동기간의 시작이 늦어지게 된다. 이는 엘니뇨 시기의 해수면온도 및 대기장 아노말리와 유사하며, 실제로 과거의 강한 엘니뇨 다음 해에는 북서태평양에서 열대저기압 활동기간의 시작일이 평년보다 늦었음을 확인하였다. 본 연구에서는 해수면온도와 북서태평양 열대저기압 활동기간 시작일 사이의 이러한 상관관계를 WRF 모델 실험을 통해 증명하고자 하였다. 실험 결과 겨울철에 인도양과 동태평양에 강한 엘니뇨 시기의 해수면온도 강제력을 주었을 때 워커순환의 약화로

인해 북서태평양 부근에 태풍 발달을 억제하는 역할을 하는 하강기류, 하층 발산 및 고기압 아노말리가 강화되었다. 이 고기압은 봄철까지 지속되어 대류를 억제하는 역할을 하였고, 그로 인해 북서태평양 열대저기압 활동기간의 시작일이 평년보다 한 달 이상 늦어졌다.

KEY WORDS: Western North Pacific 북서태평양; Tropical cyclone 열대저기압; Tropical cyclone season 열대저기압 활동 기간; sea surface temperature 해수면 온도; El Niño-Southern Oscillation (ENSO) 엘니뇨-남방진동.

Chapter 1. Introduction

Tropical cyclone (TC) is a dangerous weather phenomenon that accompanies strong winds and torrential rain. According to Park et al. (2015), TC causes extensive socio-economic damage in the coastal areas over the globe, amounting to approximately 13,600 casualties and 22 billion US dollars in losses every year. Hence, it is important to examine how the TC activity is changing with climate change to prepare for a possible damage from the TC.

The United Nations' Intergovernmental Panel on Climate Change (IPCC) suggested that climate change caused by increased anthropogenic greenhouse gas emissions can affect tropical sea surface temperature (SST) (Houghton et al. 1996). As abnormal weather phenomena associated with global warming have been remarkable during recent years, changing trend of the TC activity has been studied actively (Walsh et al., 2016). There are many studies on the changes of the TC activity in the western North Pacific (WNP) such as frequency, intensity and track (Knutson et al., 2010; Sugi et al., 2002; Chan & Liu, 2004; Wu et al., 2004). However, study on the change of the TC season is insufficient until now. Climatologically, in the WNP, TCs form throughout the year so the TC season was not so big issue. But TC season and its change is also worth in the WNP. There is no official TC season in the WNP but it may be termed the period from May to November because almost 90% of TCs form within that period.

The variability of the start of the TC season is large in the WNP. For example, in 2016, the first named TC developed on July 3. On the other hand, TC can also develop in the wintertime (January or February) like 2015.

The first named TC developed on January 13 in 2015. Even though only a few TCs form in the boreal winter (from December to February), it could cause great damage to the coastal areas. Therefore, it is necessary to examine the start of the TC season in the WNP and its change.

In this study, variation of the TC season in the WNP was analyzed. And the relationship between the TC season and the distribution of SST was examined and was proved through the model experiments.

The data used, methodology for the analysis and design of experiments are described in section 2. The variation of the TC season in the WNP for the last 64 years, the relation to large-scale environments modulating the start of the TC season and model experiments are examined in section 3. Lastly the summary and discussion are given in section 4.

Chapter 2. Data and Methods

2.1 Data

The observed TC data in the WNP is obtained from the best track data of the Regional Specialized Meteorological Centre (RSMC)-Tokyo. This data provide 6-hourly location and intensity information of TCs over the WNP from 1951 to the present. In this study, the TC formation date was defined as the day that the TC was firstly labeled as ‘tropical storm’ (i.e. TC with a maximum sustained wind speed of 17m/s) by the RSMC-Tokyo.

The large-scale environments modulating the start of the TC season were analyzed with the National Centers for Environmental Prediction (NCEP)-National Center for Atmospheric Research (NCAR) reanalysis dataset (kalnay et al., 1996).

We used the Extended Reconstructed Sea Surface Temperature (ERSST)-NOAA V3b (Smith et al., 2008) to analyze the SST distribution related to the TC season. ERSST provide monthly data from 1854 with a spatial resolution of 2° ×2° . It has relatively low resolution but can include the whole period of TC data we used. The high resolution SST data is available only from the 1980s when the satellite observation was started. So we used the Optimum Interpolation Sea Surface Temperature (OISST)-NOAA V2 (Reynolds et al., 2002), which has a high resolution for the model experiments. OISST provide weekly and monthly data from 1981 with a spatial resolution of 1° ×1° . For the model initialization, NCEP FNL (Final) Operational Global Analysis data were used. FNL data are on 1° ×1° grids

prepared operationally every 6 hours from 1999.

2.2 Definition of the TC season in the WNP

In the WNP, the lowest number of TC occurs in February (Fig.1). The number of TCs rapidly increases in May and June, and has its maximum value in August. After August, it decreases gradually until February of the following year. Thus, we newly defined ‘TC year’ which starts from February 1 when analyzing the TC season in the WNP.

For the last 64 years (1951-2014), on average, TC formation dates of the 5^{th} and 95^{th} percentile TCs are May 18 and November 28, respectively (table 1). The first date of the TC formation is April 6, 10^{th} percentile is June 13, 90^{th} percentile is November 10 and the last date is December 23. The period from the 5^{th} percentile to the 95^{th} percentile TCs is the best period that covers generally known active TC season in the WNP (i.e. from May to November). Thus, we define the TC season in the WNP as a period from the date of the 5^{th} percentile TC to the 95^{th} percentile TC in each TC year.

This definition based on the percentile considers only the effect of the temporal distribution of the annual TC occurrence, not the frequency. Also, it can remove the effects of extremely late or early TCs. Therefore, this method based on the percentile is known as a good way to define the TC season (Kossin 2008). The correlation coefficients between the TC count in each TC year and the start, end and length of the TC season is -0.12, 0.08 and 0.16, respectively. Because they are not statistically significant and the annual TC count does not affect the TC season in the WNP, we considered this definition of the WNP TC season in this study is appropriate.

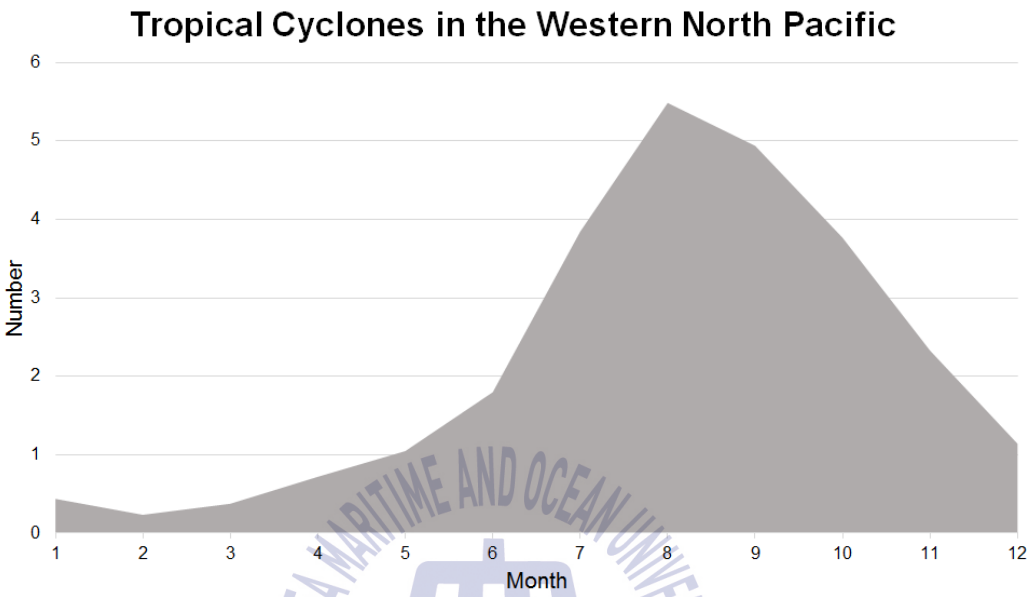

Fig. 1 Monthly mean counts of the tropical cyclones in the western North Pacific for the period from 1951 to 2014.

Table 1 Statistics for the start, end and length of the TC season over the WNP.

		Average	Standard deviation (days)	Trend (days yr^{-1})	Correlation		
Season					End	Length	Count
Start	1st TC	April 6	40.25			-0.87	
	5th percentile TC	May 18	35.81	0.26	0.17	-0.86	-0.12
	10th percentile TC	June 13	29.07			-0.83	
End	90th percentile TC	Nov 10	17.25			0.36	
	95th percentile TC	Nov 28	19.22	-0.14		0.35	0.08
	last TC	Dec 23	20.87			0.35	
Length		194.67	37.72	-0.50			0.16

2.3 model setup and experimental design

Weather Research and Forecasting (WRF) Advanced Research WRF (ARW) V3.7.1 (Skamarock et al., 2008) was used for this study. As shown in Fig. 2, we designed global WRF model with 110km horizontal resolution and nested WRF RCM with 37km horizontal resolution over the WNP region (10° S-50° N, 90° E-190° E).

The details of the model setup are given in table 2. Latitude-longitude projection was used for map projection. There are 27 vertical layers from surface to model top level (50hPa) and the time step of the model integration is 480s in the global domain and is 160s in the regional domain. And the physical parameterizations are as follows : WRF Single-moment 3-class simple ice scheme Scheme (Hong et al., 2004) for micro physics scheme, the Yonsei University scheme (Hong et al., 2006) for physics options, MM5 Similarity Scheme (Zhang & Anthes, 1982) for surface layer scheme, 5-layer Thermal Diffusion Scheme (Dudhia, 1996) for land surface scheme, the modified version of the Kain-Fritsch scheme (Kain 2004) for cumulus convection, Dudhia (1989) scheme for the short-wave radiation and Rapid Radiative Transfer Model (RRTM) scheme (Malwer et al., 1997) for the long-wave radiation.

3 experiments are carried out to determine the role of the SST distribution, affecting the TC season in the WNP (Table 3). Initialized dates are December for all experiments to reduce the impact of the model initial value. At first, 50 months (about 4 years) simulations with climatological SST (1971-2000) were carried out from December 25 as the control experiment (CNTL). And the EXP_EN experiment with SST forcing over the Indian Ocean (IO) and the Eastern Pacific (EP) was conducted 4 times with different initialized dates in December (December 4, 11, 18 and 25). We got 14 months (about 1 year) simulations from each EXP_EN experiment. Fig. 3 shows the difference in the

SST boundary conditions between the CNTL and the EXP_EN experiments. As with CNTL experiment, climatological SST were used except for the IO (20° S-20° N, 40° E-100° E) and the EP (20° S-20° N, 80° W-180° W) regions in the EXP_EN experiment. Monthly mean SSTs of strong El Niño years (1982/1983, 1997/1998) were used for those regions. Lastly, for the EXP_2016 experiment, observed 2015/2016 data were used for the model initialization and the SST boundary condition to simulate real years with strong El Nino event (2015/2016). 2015/2016 El Niño is the strongest El Niño in the last 50 years (L'Heureux et al., 2016). The EXP_2016 experiment was conducted 4 times with different initialized dates in December (2, 9, 16 and 23) like EXP_EN experiment. However, in case of 2016, there were not enough data when we conducted EXP_2016 experiment so we got only 10 months simulations from December to September. Though it is relatively short integration, late start of the TC season in the WNP simulated well enough. The ensemble averages of each result of the EXP_EN and EXP_2016 experiments were used for analysis to minimize uncertainty.

Detection and tracking algorithm for simulated TCs used in this study is same as those described in Zhao et al. (2009) :

- Storm center defined as local minimum of sea level pressure within 2° of 850hPa relative vorticity which must be higher than $3.5 \times 10^{-5} s^{-1}$
- The local maximum of temperature averaged between 300 and 500hPa within 2° of storm center is warm-core center and it must be at least 1K warmer than the surrounding local mean.
- The initial point of storm trajectory must be located between 40° S and 40° N
- The distance between two consecutive storms in 6 hour intervals must be less than 400km

- The trajectory must last at least 3 days with the maximum surface wind speed greater than 17m/s (not necessarily successive).

Table 2 Model configuration and Parameterization schemes used in the WRF model experiments

Model	WRF-ARW
Map projection	Latitude-longitude
Number of vertical levels	27
Time step	480s / 160s
Micro physics scheme	WRF Single–moment 3–class
Physics Options	Yonsei University Scheme (YSU)
Surface layer scheme	MM5 Similarity Scheme
Land surface scheme	5–layer Thermal Diffusion Scheme
Cumulus parameterization scheme	Kain–Fritsch Scheme
Short-wave radiation scheme	Dudhia Shortwave Scheme
Long-wave radiation scheme	RRTM Longwave Scheme

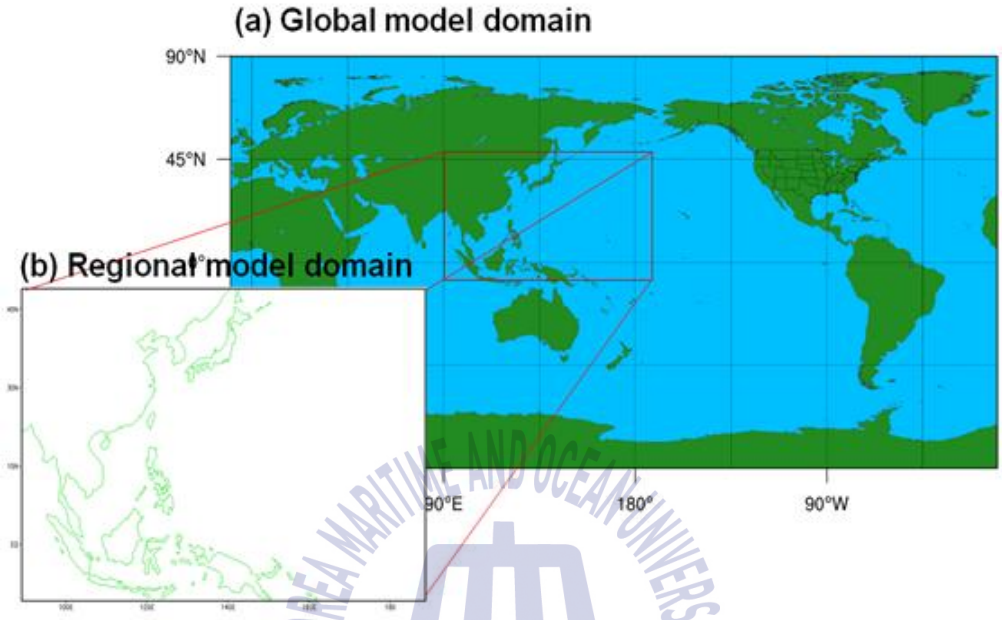

Fig. 2 (a) Global and (b) regional model domains.

Table 3 Design of experiments. IO and EP denote the Indian Ocean (20° S-20° N, 40° E-100° E) and the East Pacific (20° S-20° N, 80° W-180° W), respectively.

Experiments	Year	SST boundary condition	Ensemble No.	Initialized date
CNTL	2002-2006	Climatological OISST (1971-2000)	1	25 Dec
EXP_EN	2002-2003	Climatological OISST (1971-2000) + OISST of mean SST of strong El Niño Years (1982/1983, 1997/1998) in the IO and the EP	4	04,11,18,25 Dec
EXP_2016	2015-2016	OISST of simulating years (2015, 2016)	4	02,09,16,23 Dec

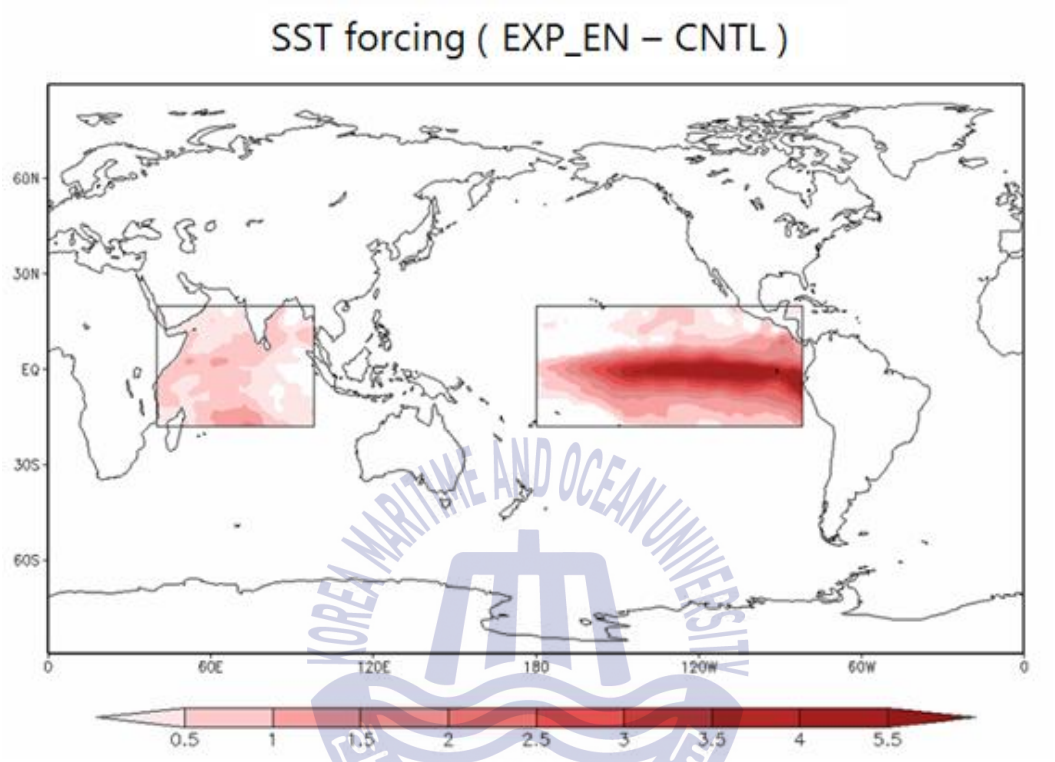

Fig. 3 Difference in SST boundary conditions between EXP_EN and CNTL experiments.

Chapter 3. Results

3.1 Variation of the TC season in the WNP

Fig. 4 shows the box-whisker plots for annual TC formation dates during the period from 1951 to 2014 based on the TC year. The boxes cover from 25^{th} to 75^{th} percentiles of annual TC formation dates and whiskers are extended to the 5^{th} and 95^{th} percentiles of annual TC formation dates representing the TC season. The first and last TC formation dates are also marked with dots. Lower and upper red lines indicates that linear trend for the last 64 years of the 5^{th} and 95^{th} percentile TC formation dates, respectively. Both the start and the end dates have interannual and long-term variation. In the long-term, As shown in Table 1, the start date of the TC season has delayed (0.26 days yr^{-1}) while the end date has become earlier (-0.14 days yr^{-1}), representing that the length of the TC season is getting shorter (-0.50 days yr^{-1}). However, these long-term trends are not statistically significant at the 90% confidence level.

As shown in Fig.4, the TC season in the WNP show apparent interannual variability. The standard deviation and correlation coefficient for interannual variation of the parameters for TC season are listed in Table 1. The standard deviations of the start date, end date and the length of the TC season are 35.81, 19.22 and 37.72 days, respectively. The start date and the length of the TC season in the WNP have large interannual variations more than a month while the variation of the end date of the TC season is relatively small, and it is also seen in Fig.4. The correlation coefficient between the length and

the start date is -0.86, the length and the end date is 0.35, the start and the end date is 0.17. These results indicate that the length of the TC season is highly dependent on its start date rather than its end date. And the start and the end of the TC season is not dependent on each other.

Due to the weak signal in the long-term trends, we paid attention to interannual variation of the TC season in the WNP. Also, because the start date of the TC season is a main factor modulating the variation of the TC season, we focused on the start date of the TC season.

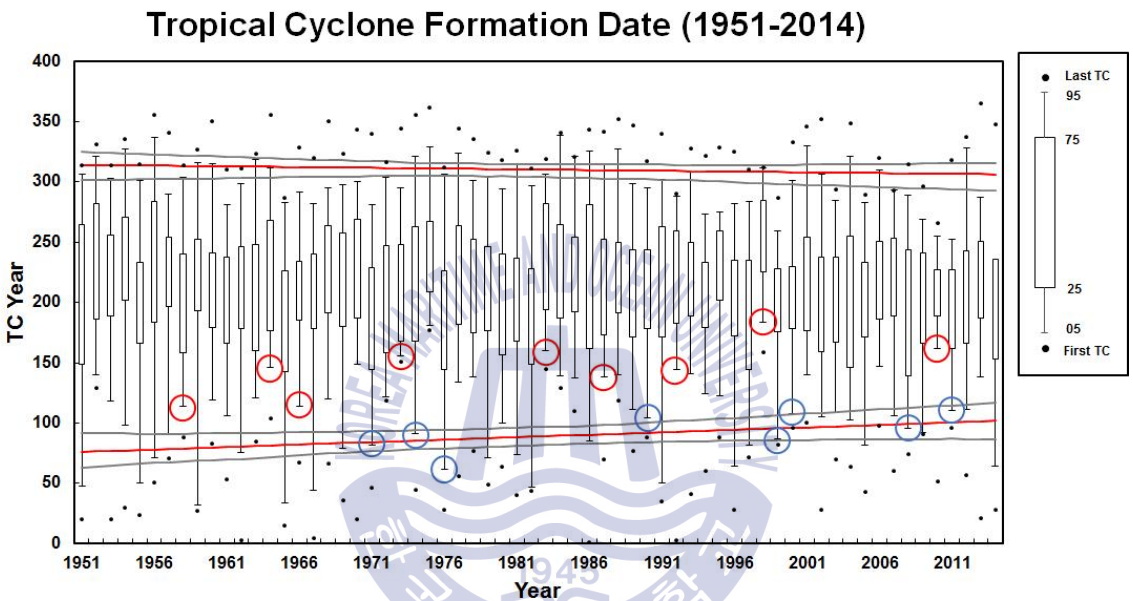

Fig. 4 Box-whisker plots for the WNP TC formation dates for 1951-2014. The boxes cover from 25th to 75th percentiles of annual TC formation dates and whiskers are extended to the 5th and 95th percentiles of annual TC formation dates. The first and last TC formation dates are marked with dots. Red lines denote linear trends for the periods 1951-2014 of the 5th and 95th percentiles. Gray lines denote 95% confidence interval. Red and Blue circles indicate the 5th percentile TC formation dates in the following year of the El Niño and La Niña events, respectively.

3.2 Large-scale environments modulating the start of the TC season in the WNP

Fig. 5 shows the correlation between the start date of the TC season in the WNP and large scale environments modulating the TC activity (SST, 850hPa geopotential height, zonal stream function) during the period from 1951 to 2014. In Fig. 5, the positive (negative) correlation means that the start of the TC season is relatively late (early) when environments anomalies are positive (negative).

As shown in Fig. 5ab, relative distribution of SST is highly correlated with the start of the TC season in the WNP. Sufficiently warm SST is one of requirements for the TC formation. TC can form over tropical seas when SST is over 26° C and SST on the TC track is the main factor that control TC activity. There are high positive correlations which are close to 0.4 in the IO and the EP and negative correlation in the east side of the western Pacific (WP) in the preceding winter and the following spring. It means that the start of the TC season is delayed when the IO and the EP are warm and the eastern WP is cool in the preceding winter.

Not only SST over the WNP, but high SST over the equatorial eastern Pacific increases the average TC activity in the WNP (Chan & Liu, 2004). Actually, this SST pattern in Fig. 5ab associated with ENSO (Harrison & Larkin, 1998). Many previous studies have suggested that ENSO-like SST anomalies over tropics cause anomalous anticyclone over the WNP. The anticyclonic flow develops in the Philippine Sea during the boreal winter of El Niño phase and is sustained until the following spring by a Rossby waves response to El Niño induced subsidence over the Maritime Continent and an increase in westerly over the tropical WP which are forced by the SST warming over the central-eastern Pacific (Wang et al., 2000; Wang & Zhang,

2002; Wu et al., 2010b). As well as the process in the tropical Pacific sector, the El Niño-related warm SST anomalies over the IO also intensify and sustain the anomalous Philippine Sea anticyclone by a Kelvin wave response that forces surface divergence and descent over the WNP (Watanabe & Jin, 2002; Lau & Nath, 2003; Annamalai et al., 2005; Yang et al., 2007; Yuan et al., 2012; Wu et al., 2010a; Du & Yang, 2011). This macanism is shown in Fig. 5c-f. Anomalous anticyclone is located over the WNP in the winter (Fig. 5c) and lasts until the spring (Fig. 5d). Fig. 5ef show weakened Walker circulation and resulting surface divergence and descent over the WNP.

Thus, the correlation patterns shown in Fig. 5 can be interpreted as a results from a similar physical process as the aforementioned ENSO-related variations and is linked to the late start of the TC season. So we examined this relationship between ENSO and the start of the TC season using Niño3.4 index (Table 4). We define El Niño (La Niña) if the Niño3.4 index is over 1 standard deviation greater (less) than preceding winter from December to February. The mean start date of the TC season following strong El Niño event is June 21 while one following strong La Niña is May 5. The mean start date of the TC season following El Niño is delayed more than one and a half month from the mean start date of the TC season after La Niña, and that is statistically significant at the 99% confidence level. In Fig. 4, red (blue) circles indicate the start date of the TC season in the following year of the strong El Niño (La Niña) events. When the El Niño (La Niña) was strong in the winter, the start of the following TC season was obviously late (early). This result confirms that the TC season in the WNP is significantly modulated by El Niño-related SST variations.

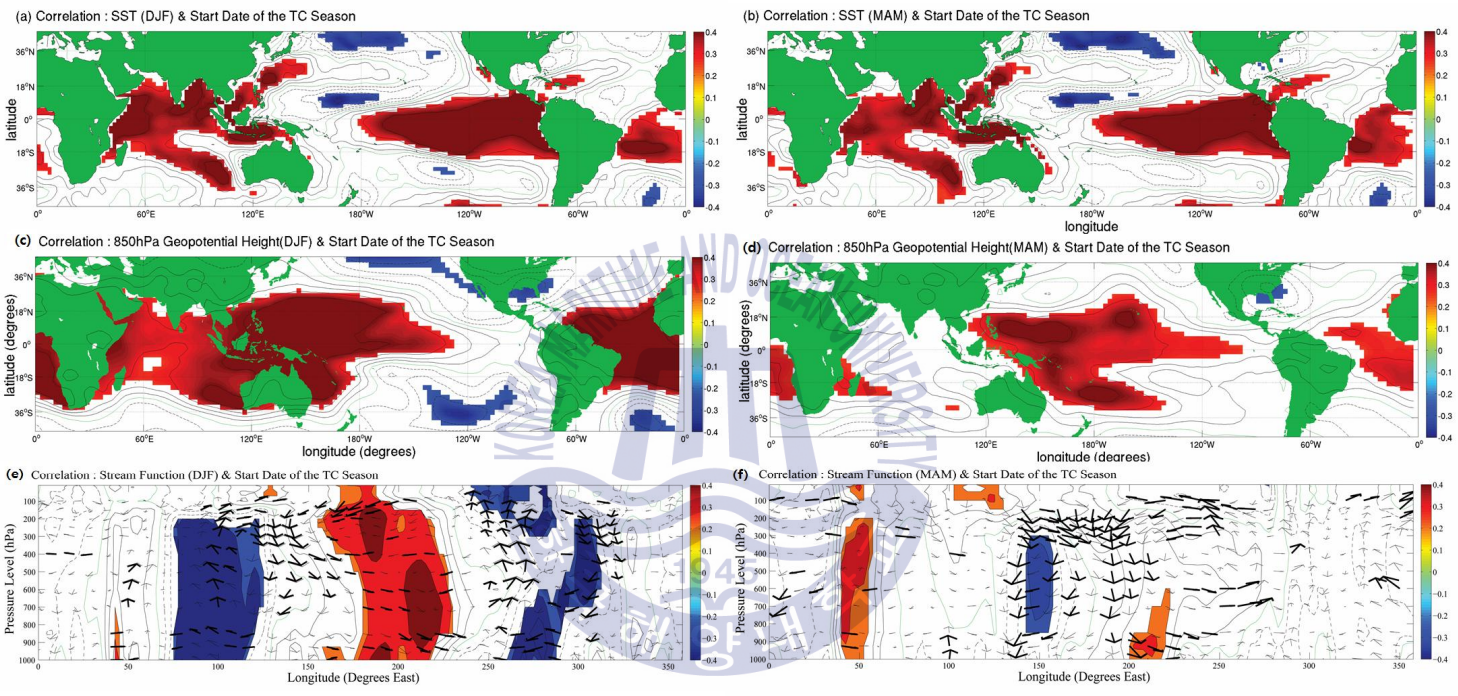

Fig. 5 The correlation coefficients between the start date of the TC season and (a,b) SST , (c,d) 850hPa geopotential height and (e,f) zonal stream function (averaged from 0° to 20° N). The left panels show correlation coefficients in the preceding winter (December-February) and the right panels show them in the following spring (March-May). The Solid lines and dashed lines denote positive and negative values, respectively, and green lines denote zero. The shading and thick vectors indicate the significance more than 95% confidence level.

Tabel 4. The start dates of the TC season following the strong ENSO events in the preceding winter. The ordinal date is the count of days from February 1.

El Niño	TC Year	1958	1964	1966	1973	1983	1987	1992	1998	2010	Mean
	Ordinal Date	118	139	110	156	160	139	145	178	124	141
	Calendar Date	May 29	June 9	May 21	July 6	July 10	June 19	June 25	July 28	June 4	June 21
La Niña	TC Year	1971	1974	1976	1989	1999	2000	2008	2011		Mean
	Ordinal Date	79	90	66	108	89	113	97	110		94
	Calendar Date	April 20	May 1	April 7	April 19	April 30	April 24	May 8	May 21		May 5

3.3 Results of model experiments

WRF model experiments are conducted to examine how the SST distribution affect the start of the TC season. Fig. 6 shows distributions of monthly TC occurrences for observations, CNTL and EXP_EN experiments. Distributions of simulated TCs for observation and CNTL experiment are very similar to each other that have their maximum (minimum) number in August (February). Table 5 shows statistics of the TC season in the WNP for observation and simulations. The mean start date, end date, Length and number of the TC season for the CNTL experiment are May 23, December 1, 192 days and 26.75 respectively. It is also similar to observation (May 18, November 28, 195 days and 26.11) so results of WRF experiments in this study are considered reliable.

On the other hand, in case of EXP_EN experiment, the start date of the TC season is June 27 and it is more than a month later than CNTL experiment. The number of annual TC is 24.67 which is less than CNTL experiment. As shown in Fig. 6, Some TCs developed before May and the number of TCs increases since April and May for the CNTL experiment. However, there are hardly any TCs before May and the TC occurrence rapidly increases after May and June for the EXP_EN experiment. The TCs simulated in the EXP_2016 experiment also show similar distribution with EXP_EN (Fig. 7). 2015/2016 El Niño was the strongest El Niño and the start of the TC season in the WNP was extremely late in 2016. There are no TCs before May and the first TC is developed in June. It was not possible to calculate the start date of the TC season for the EXP_2016 experiment because integration period was only until September. But the first TC simulated in the EXP_2016 was developed on June 6 and as shown in Table 1, it is two months later than the date of the average first TC for the last

64 years (April 6). It is also about a month later than the first TC simulated in the CNTL experiment (April 24). Thus, model experiments proved that ENSO-like SST anomalies (i.e. anomalous warm SST over the IO and the EP) in the preceding winter cause the start of the TC season in the WNP to be delayed.

In order to investigate the mechanism of this relationship, we analyzed differences in the simulated atmospheric circulation between EXP_EN and CNTL experiments. Fig. 8 illustrates differences in 850hPa geopotential height, relative vorticity and horizontal winds between EXP_EN and CNTL experiments. Anomalous anticyclone developed during the winter is illustrated in Fig. 8a. It is diminished in spring but is still sustained over the WNP and plays a role in suppressing TC genesis (Fig. 8b). 850hPa relative vorticity and horizontal winds show negative relative vorticity and anticyclonic circulation over the WNP in the winter and the following spring (Fig. 8c-f). As shown in Fig. 5, these signals in Fig. 8 have positive correlation with the start of the TC season in the WNP. It implies that when the SST forcing is given over the IO and the EP in the winter, anomalous anticyclone is developed over the WNP in the winter and the following spring and it causes the start of the TC season to be late.

Table 5 Statistics of the TC season for observations (1951–2014) and simulations.

TC season	Observation (1951-2014)	Simulation	
		CNTL	EXP_EN
Start date	May 18	May 23	Jun 27
End date	Nov 28	Dec 1	Nov 14
Length	195 days	192 days	140 days
Number	26.11	26.75	24.67

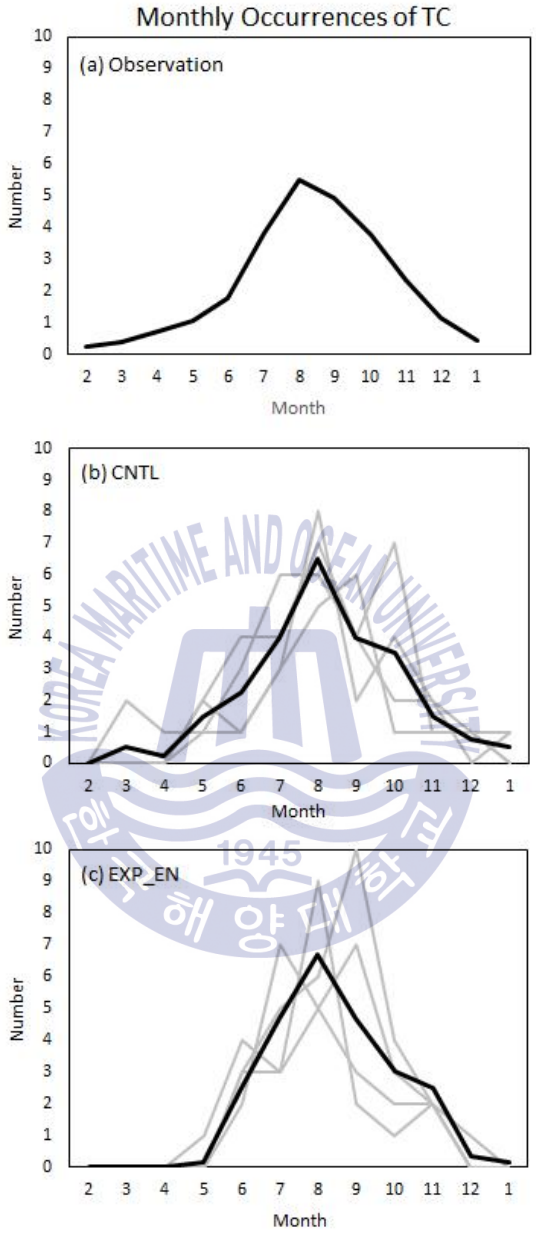

Fig. 6 Distribution of monthly mean TCs in the WNP for (a) observations (1951-2014) and (b,c) experiments. Grey lines denote that each model experiment and black lines indicate ensemble mean of them.

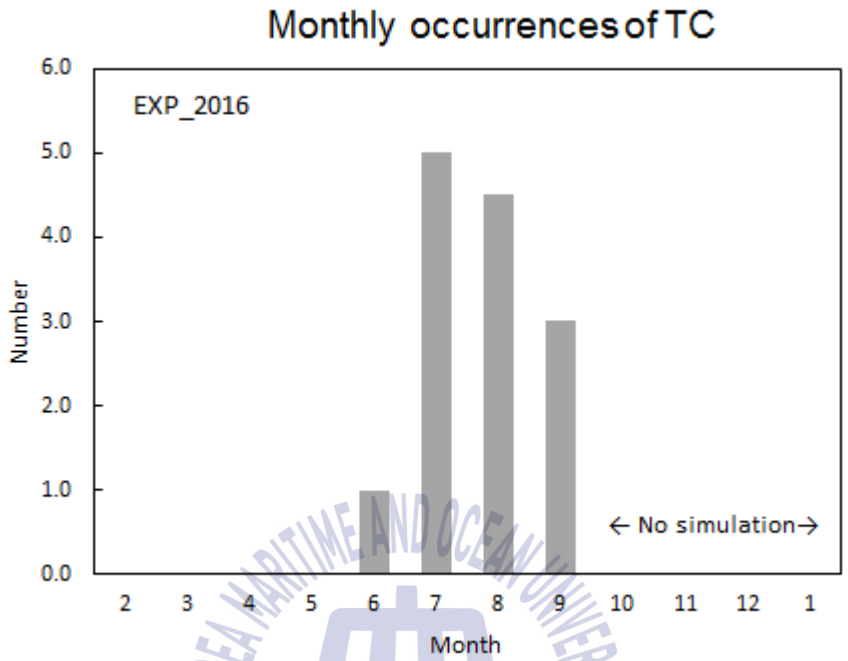

Fig. 7 Distribution of monthly mean TC for EXP_2016 experiment.

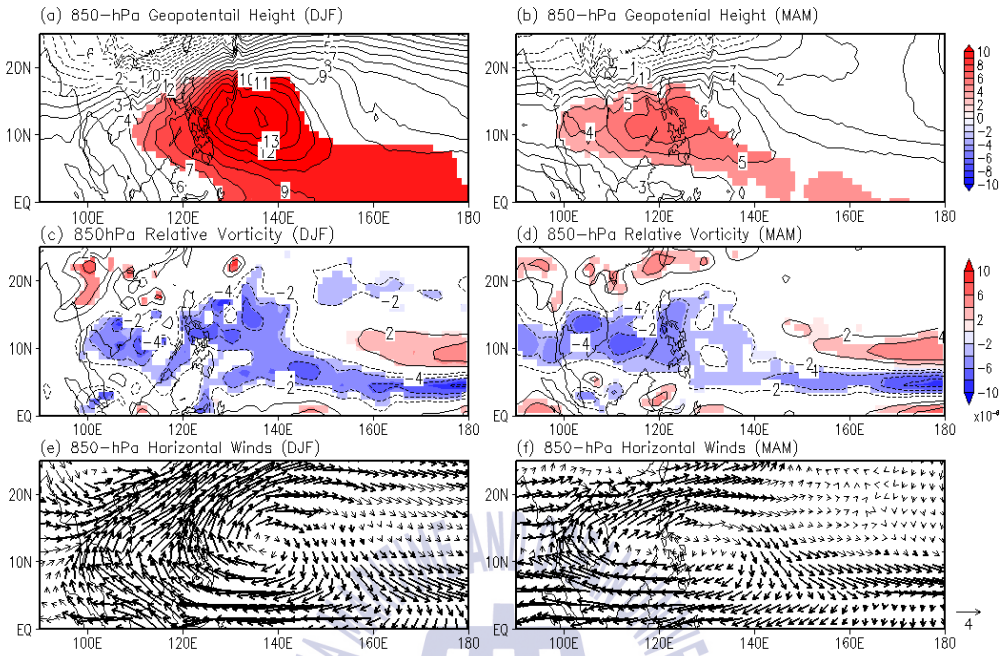

Fig. 8 Differences in (a, b) 850hPa geopotential height, (c, d) relative vorticity, (e, f) horizontal winds from EXP_EN and CNTL. (EXP_EN minus CNTL). The left panels show the differences in the environments from December to February and the right panels show them in March to May. The shading and thick vectors indicate the significance at the 90% confidence level.

Chapter 4. Summary and Discussion

In the WNP, the TC season depend heavily on its start date which have large interannual variation and the start date controlled by SST over the IO and the EP. ENSO-like SST anomalies (i.e. anomalous warm SST over the IO and the EP) weaken Walker circulation and induce surface divergence and descent over the WNP which is the TC formation region. It causes anomalous anticyclone over the WNP in the winter and this anomaly lasts until the spring. This mechanism plays a role in inhibiting the TC formation by suppressing convection. As a result, the start of the TC season in the WNP is delayed and the length of the season which is rely on its start becomes shorter. It implies that not only local SST warming, but also tropical SST distribution is important factor to predict TC activity in the WNP.

In terms of long-term variation, as mentioned in section 3.1, the TC season in the WNP getting shorter for the last 64 years with the delay of its start. But actually, though global SST is rising due to the global warming, TC season in the WNP have been delayed less than expected. The start date of the TC season is delayed about 0.26 days a year (Table 1) and this trend is not statistically significant. Although the long-term trends are insignificant and weak, it is notable because it contrasts with the trend of the hurricane season (Kossin, 2008). Kossin (2008) suggested that the hurricane season is getting longer, as the dates of occurrence of the first and last hurricanes have decreasing and increasing trend, respectively. Local SST warming in the hurricane developing region is interpreted as the reason. However, in case of TC in the WNP, local SST does not affect the length of the TC season. TC

activity in the WNP is associated to the remote SST variations and related atmospheric conditions over the WNP. But due to the large uncertainty in the insignificant long-term variation of the TC season in the WNP, unfortunately, the environmental factors that affect the long-term variation of the TC season in the WNP remain unknown.

Acknowledgments

2014년 3월, 많은 걱정을 안고 석사과정을 시작했었는데 어느새 이렇게 졸업을 하게 되었습니다. 졸업을 하기까지 많은 분들의 도움이 있었지만 가장 먼저 부족한 점 많았던 첫 제자를 처음부터 하나 하나 지도해 주신 김형석 교수님께 감사드립니다. 연구실 선배가 없어 교수님께 직접 여쭤볼 수밖에 없었는데, 교수님께서 잘 이끌어주신 덕분에 짧은 대학원 생활 동안 많은 것을 배우고 성장할 수 있었습니다. 입학을 하고 나서도 잘 해낼 수 있을지 걱정과 고민이 많았지만, 항상 모자란 것 보다는 잘한 것부터 봐주시고 격려해주신 덕분에 이렇게 졸업까지 올 수 있었습니다.

또한 학부 때 대기과학을 공부하여 해양 분야는 전혀 모르던 저에게 많은 가르침을 주신 이호진 교수님과 이경은 교수님께 감사드립니다. 해양 분야 대학원 수업이 힘들기도 했지만 교수님들께서 잘 가르쳐 주신 덕분에 극지해양과 고해양학 분야에도 흥미를 가지게 되었고 재미있게 수업을 들었습니다. 같이 수업을 들으며 제게 도움을 주셨던 미옥 언니와 상엽 오빠, 은선이, 령아에게도 감사합니다. 제 논문에 대해 다양한 조언과 함께 정성 어린 심사를 해주신 박두선 박사님께도 감사드립니다.

학회에 갈 때 마다 연구실 동료가 없는 저를 챙겨주신 UNIST의 기후환경모델링 연구실(UCEM) 학생분들과 이명인 교수님, 박명숙 박사님께도 감사드립니다. 특히 항상 같은 방을 쓰며 언니처럼 챙겨주고 많은 조언을 해주신 혜림 언니에게 감사하다는 말씀 드리고 싶습니다.

처음 연구실에 들어와서 혼자 외로울 무렵 연구실에 들어온 형석이와 소진이, 그리고 2년 동안 같은 방에 살았던 예은이에게도 고맙습니다. 덕분에 외롭지 않게 대학원 생활을 할 수 있었습니다.

마지막으로 언제나 믿어주시고 응원해주시는 부모님과 할머니 할아버지, 든든한 동생에게 감사하며 이렇게 고마운 분들을 생각하며 앞으로 더욱 발전하는 사람이 되도록 하겠습니다.

References

Annamalai, H., P. Liu, and S. Xie, 2005. Southwest Indian Ocean SST Variability: Its Local Effect and Remote Influence on Asian Monsoons. *J. Climate*, 18, 4150-4167, doi: 10.1175/JCLI3533.1.

Chan, J. C. L., and K. S. Liu, 2004. Global warming and western North Pacific typhoon activity from an observational perspective. *J. Climate,* 17, 4590-4602

Du, Y., L. Yang, and S. P. Xie, 2011. Tropical Indian Ocean Influence on Northwest Pacific Tropical Cyclones in Summer following Strong El Nino. *J Climate*, 24, 315-322.

Dudhia, J., 1989. Numerical study of convection observed during the winter monsoon experiment using a mesoscale two dimensional model. *J. Atmos. Sci.* 46, 3077-3107.

Dudhia, J., 1996: A multi-layer soil temperature model for MM5. Preprints, The Sixth PSU/NCAR Mesoscale Model Users' Workshop, Boulder, CO, Natl. Ctr. *Atmos. Res.*

Harrison, D. E., and N. K. Larkin, 1998. El Nin˜o-Southern Oscillation sea surface temperature and wind anomalies, 1946-1993. *Rev. Geophys.,* 36, 353-400.

Hong, S., J. Dudhia, and S. Chen, 2004. A Revised Approach to Ice Microphysical Processes for the Bulk Parameterization of Clouds and Precipitation. *Mon. Wea. Rev.,* 132, 103-120, doi: 10.1175/1520-0493(2004)132<0103:ARATIM>2.0.CO;2.

Hong, S., Y. Noh, and J. Dudhia, 2006. A New Vertical Diffusion Package with

an Explicit Treatment of Entrainment Processes. *Mon. Wea. Rev.*, 134, 2318-2341, doi: 10.1175/MWR3199.1.

Houghton, J. T., L. G. Meira Filho, B. A. Callander, N. Harris, A. Kattenberg, and K. Maskell, 1996. Climate change 1995: The science of climate change. Contribution of working group I to the second assessment of the Intergovernmental Panel on Climate Change. *Cambridge university Press,* 572pp.

Kain, J.S., 2004. The Kain-Fritsch convective parameterization: An update. *J. Appl. Meteor.* 43, 170-181

Kalnay, E., and Coauthors, 1996. The NCEP/NCAR 40-Year Reanalysis Project. *Bull. Amer. Meteor. Soc.*, 77, 437-471.

Knutson TR, McBride JL, Chan J, Emanuel K, Holland GJ, Landsea CW, Held CI, Kossin JP, Srivastava AK, Sugi M, 2010. Tropical cyclones and climate change. *Nat Geosci* 3:157-163

Kossin, J. P., 2008. Is the North Atlantic hurricane season getting longer?. *Geophys Res Lett., 35.*

Lau, N. and M. Nath, 2003. Atmosphere-Ocean Variations in the Indo-Pacific Sector during ENSO Episodes. *J. Climate*, 16, 3-20, doi: 10.1175/1520-0442(2003)016<0003:AOVITI>2.0.CO;2.

L'Heureux , M. L., and Coauthors, 2016. Observing and predicting the 2015-16 El Nino. *Bull. Amer. Meteor. Soc.*, doi:10.1175/BAMS-D-16-0009.1.

Mlawer, E.J., S.J. Taubman, P.D. Brown, M.J. Iacono, S.A. Clough, 1997. Radiative Transfer for inhomogeneous atmospheres: RRTM, a validated correlated-k model for the longwave. *J. Geophys. Res.* 102, 16,663-16,682.

Park, D-S. R., C.-H. Ho. C. C. Nam, and H.-S. Kim (2015) Evidence of adaptation effectiveness on tropical cyclones in Republic of Korea,

Environmental Research Letters., 10, 054003.

Reynolds, R. W., N. A. Rayner, T. M. Smith, D. C. Stokes, and W. Wang, 2002. An improved in situ and satellite SST analysis for climate. *J. Climate,* 15, 1609-1625, doi:10.1175/1520-0442(2002)015,1609: AIISAS.2.0.CO;2

Skamarock, W. C., and Coauthors, 2008. A description of the Advanced Research WRF version 3. *NCAR Tech. Note* NCAR/TN-475+STR, 113 pp.

Smith, T. M., Reynolds, R. W., Peterson, T. C. and Lawrimore, J., 2008. 'Improvements to NOAA's Historical Merged Land-Ocean Surface Temperature Analysis (1880-2006).' *J. Climate,* 21: 2283-2296.

Sugi, A. Noda, and N. Sato, 2002. Influence of the global warming on tropical cyclone climatology: An experiment with the JMA global model. *J. Meteor. Soc. Japan,* 80, 249-272

Walsh, K. J.E., McBride, J. L., Klotzbach, P. J., Balachandran, S., Camargo, S. J., Holland, G., Knutson, T. R., Kossin, J. P., Lee, T.-c., Sobel, A. and Sugi, M., 2016. Tropical cyclones and climate change. *WIREs Clim Change*, 7: 65-89. doi:10.1002/wcc.371

Wang, B., R. Wu, and X. Fu, 2000. Pacific-east Asian teleconnection: How does ENSO affect east Asian climate?, *J. Climate*, 13(9), 1517 - 1536.

Wang, B., and Q. Zhang, 2002. Pacific-East Asian teleconnection. Part II: How the Philippine Sea anomalous anticyclone is established during El Niño development. *J. Climate*, 15:3252-3265.

Watanabe, M., and F.-F. Jin, 2002. Role of Indian Ocean warming in the development of Philippine Sea anticyclone during ENSO. *Geophys Res Lett,* 29:1478.

Wu, L., and B. Wang, 2004. Assessing impacts of global warming on tropical cyclone tracks. *J. Climate*, 17, 1686-1698.

Wu, B., T. Li, and T. Zhou, 2010a. Asymmetry of Atmospheric Circulation Anomalies over the Western North Pacific between El Niño and La Niña. *J. Climate,* 23, 4807-4822, doi: 10.1175/2010JCLI3222.1.

Wu, B., T. Li, and T. Zhou, 2010b. Relative Contributions of the Indian Ocean and Local SST Anomalies to the Maintenance of the Western North Pacific Anomalous Anticyclone during the El Niño Decaying Summer. *J. Climate*, 23, 2974-2986, doi: 10.1175/2010JCLI3300.1.

Yang, J., Q. Liu, S.-P. Xie, Z. Liu, and L. Wu, 2007. Impact of the Indian Ocean SST basin mode on the Asian summer monsoon, *Geophys. Res. Lett.*, 34, L02708, doi:10.1029/2006GL028571.

Yuan, Y., S. Yang, and Z. Zhang, 2012. Different Evolutions of the Philippine Sea Anticyclone between the Eastern and Central Pacific El Niño: Possible Effects of Indian Ocean SST. *J. Climate*, 25, 7867-7883, doi: 10.1175/JCLI-D-12-00004.1.

Zhang, D. and R. Anthes, 1982: A High-Resolution Model of the Planetary Boundary Layer—Sensitivity Tests and Comparisons with SESAME-79 Data. *J. Appl. Meteor.*, 21, 1594-1609, doi: 10.1175/1520-0450(1982)021<1594:AHRMOT>2.0.CO;2.

Zhao, M., and I. M. Held, S. -J. Lin, and G. A. Vecchi, 2009. Simulations of global hurricane climatology, interannual variability, and response to global warming using a 50-km resolution GCM. *J. Climate*, 22, 6653-6678, doi:10.1175/2009JCLI3049.1.